02

Photoluminescence of sapphire irradiated by low-energy electrons and ions

© E.Yu. Zykova, K.E. Ozerova, A.A. Tatarintsev, A.N. Turkin

Lomonosov Moscow State University,
119992 Moscow, Russia

e-mail: zykova@phys.msu.ru

Photoluminescence (PL) of sapphire single crystals as received and preirradiated by low energy Ar^+ ions and electrons has been studied to reveal a relationship between sapphire charging under electron beam irradiation and radiation-induced defect formation. The photoluminescence spectra were obtained using a confocal microscope excitation wavelength of 445 nm as well as by a nonconfocal method with excitation at a wavelength of 355 nm. The lines observed in PL spectra for all samples are associated with both intrinsic and impurity defects. It has been established that preliminary ion irradiation leads to disordering of the near-surface region of the sample resulting in a significant increase in the photoluminescence intensity. Preliminary electron irradiation can lead to a change in the charge state of defects that initially exist in the crystal.

Keywords: radiation-stimulated defects, sapphire photoluminescence, ion and electron irradiation.

Introduction

Sapphire, the single-crystalline α-Al_2O_3, is widely used in many areas — optics and microelectronics, heterogeneous catalysis and dosimetry. In various technical applications it is exposed to charged particles — electrons, ions and protons. Since sapphire is a dielectric, that conducts electricity poorly (its resistivity is 10^{16} Ω·cm at $T = 25°C$), its irradiation with charged particles of low and medium energies leads to the accumulation of an electric charge in the near-surface region, as a result of which a negative or positive potential appears on the surface. The charging of the crystal surface in many cases is a negative factor leading to the appearance of strong internal fields and even to electrical breakdown.

In previous experiments [1–3] on the study of the kinetics of charging dielectric massive single-crystalline samples of sapphire and quartz, it was found that the surface potential of sapphire begins to grow only a few minutes after switching-on the electron irradiation. Moreover, the start time of sample charging depended both on the energy and on the current density of the irradiating electrons. For the incident electron energy $E_0 = 15$ keV, for example, it was ~ 20 min. At the same time the charging kinetics of a single-crystal quartz sample had a different character: the surface of single-crystalline quartz began to be negatively charged almost immediately after the electron beam was switched on, and the time to reach the equilibrium charge potential was 30 s. To explain this fact, it was suggested that the charging kinetics is largely determined by the number of electron traps (defective or impurity nodes) both initially existing in the crystal and created in the crystal by electron irradiation itself.

It was assumed that initially the sapphire sample has a very small number of defects, so it does not charge. However, in the process of electron irradiation, radiation defects can form in the near-surface layer of the dielectric, which serve as traps for primary electrons. With the accumulation of such radiation defects in a sapphire sample, the capture of injected electrons on the created traps begins, that determines the observed kinetics of surface charging and the time it takes to establish the equilibrium potential.

The assumptions put forward were confirmed by the experimentally observed fact that after preliminary irradiation of the samples with electrons and low-energy ions, the sapphire began to charge immediately after switching-on the electron irradiation [1,2], that can be explained by the fact that the preliminary irradiation creates radiation defects in the sample near-surface region, which intensively capture the injected electrons.

At present luminescent research methods are successfully used to control the degree of stoichiometry and purity of materials, the presence of electrically active and inactive impurities and defects in them. Luminescence spectra contain information about the mechanisms of radiative recombination in an object, that allows obtaining detailed information about the nature of defects, their distribution over the surface and volume of the material, as well as radiation-induced changes.

The purpose of this study was to study the changes occurring in the sapphire near-surface region under the effect

of electrons and low-energy ions using a photoluminescence (PL) method.

Samples and experimental procedure

For the experiments we used polished single-crystalline sapphire samples with a thickness of 0.33 mm and lateral dimensions of 10×5 mm, produced by Monocrystal (Russia). Three samples were studied: sample № 1 — initial sample Al_2O_3, two other samples were preliminarily irradiated in high vacuum conditions ($p \sim 10^{-8}$ Torr) at room temperature by low-energy electrons and ions, respectively. Electron irradiation was carried out in the ultrahigh-vacuum chamber of the Varian Auger spectrometer, using an electron gun with the following parameters: the size of the electron beam on the sample was $0.3-3$ mm, depending on the operating mode; electron energy 300 eV-3 keV; current — from 0.4 to 200μA. Sample № 2 was irradiated with electrons with energy $E_{el} = 2$ keV and electron beam current $I = 50 \mu$A, and the irradiation region had an elliptical shape with dimensions of $3-4$ mm, irradiation time $t_{el} = 120$ min, fluence $2 \cdot 10^{19}$ el/cm^2. Sample № 3 — Al_2O_3 irradiated with Ar$^+$ ions. Irradiation was carried out in a vacuum facility equipped with an Ardenne duoplasmatron at a residual pressure of 10^{-6} Torr. Ion energy $E_{ion} = 9$ keV, ion beam current $I_{ion} = 40 \mu$A, irradiation region $\varnothing 4$ mm, exposure time 30 min.

The PL spectra were measured using Ntegra Spectra NT-MDT confocal microscope at an excitation wavelength of $\lambda = 445$ nm with a laser pulse duration of FWHM < 80 ps. The use of laser confocal microscopy allowed to detect radiation only from the near-surface layer of the sample with a thickness of no more than 2μm, that minimized the effect of the unirradiated part of the crystal. In addition, the PL spectra were recorded in a standard (non-confocal) geometry at an excitation wavelength of 355 nm (pulse duration 6 ns) using a Shamrock SR303i spectrometer, in which Andor DU420A CCD camera was used to record radiation.

Experimental results and discussion

PL spectra upon excitation at a wavelength $\lambda_{ex} = 355$ nm
Figure 1 shows the PL spectra of single-crystalline samples Al_2O_3 obtained upon excitation by a laser with a wavelength of $\lambda_{ex} = 355$ nm. The curve *1* (black) represents the PL spectrum of the initial sample, the curves *2* (red) and *3* (green) — spectra from the samples previously irradiated with electrons and ions, respectively Ar$^+$.

The narrow intense line observed in the PL spectrum in the Fig. 1 at the wavelength $\lambda = 693$ nm consists of two narrow bands and is a well-known doublet of Cr^{3+} R lines. It is known that chromium, iron, magnesium and some other elements can be present in Al_2O_3 crystals
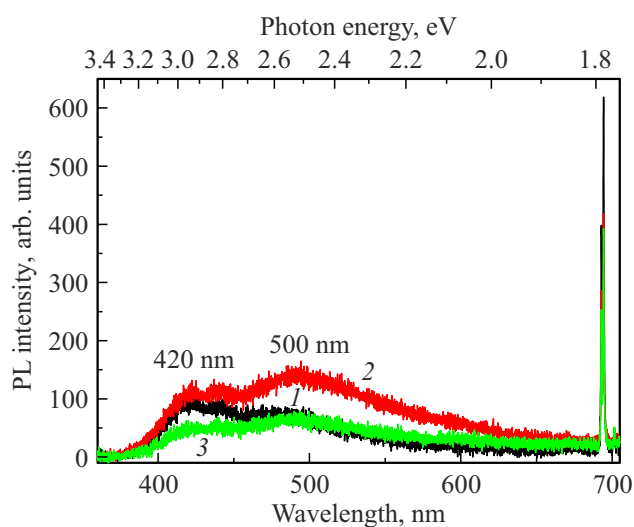

Figure 1. Panoramic spectra of PL samples α-Al_2O_3 taken at laser excitation wavelength $\lambda = 355$ nm. Curve *1* — initial sapphire sample, *2* — sample pre-irradiated with electrons, *3* — sample after irradiation with Ar$^+$ ions.
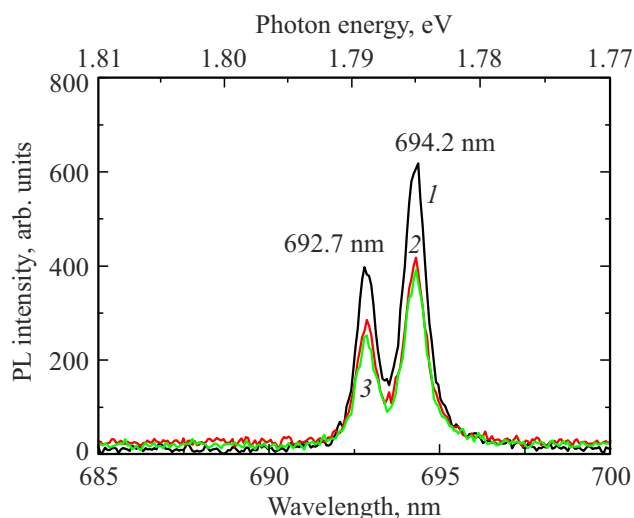
Figure 2. Luminescence R_1- and R_2 lines of Cr^{3+} ions in crystals Al_2O_3. Curve *1* — initial sapphire sample, *2* — sample pre-irradiated with electrons, *3* — sample after irradiation with Ar$^+$ ions.

in low concentrations ($< 10^{-3}$ mas %) as natural impurities [4]. Some of these uncontrolled impurities, in particular chromium and titanium, can significantly affect the optical and luminescent properties of sapphire monocrystals, even at low concentrations. The Figure 2 shows the lines R_1- and R_2 separately on a larger scale, the positions of which in the sapphire PL spectrum correspond to the wavelengths $\lambda_{max} = 692.7$ nm and $\lambda_{max} = 694.2$ nm. These lines are well studied and correspond to the transition $^2E \rightarrow ^4A_2$ in Cr^{3+} ions replacing Al^{3+} ions in a sapphire lattice.

It should be noted here that the intensity of the R lines in the samples preliminarily irradiated with electrons (curve *2*)
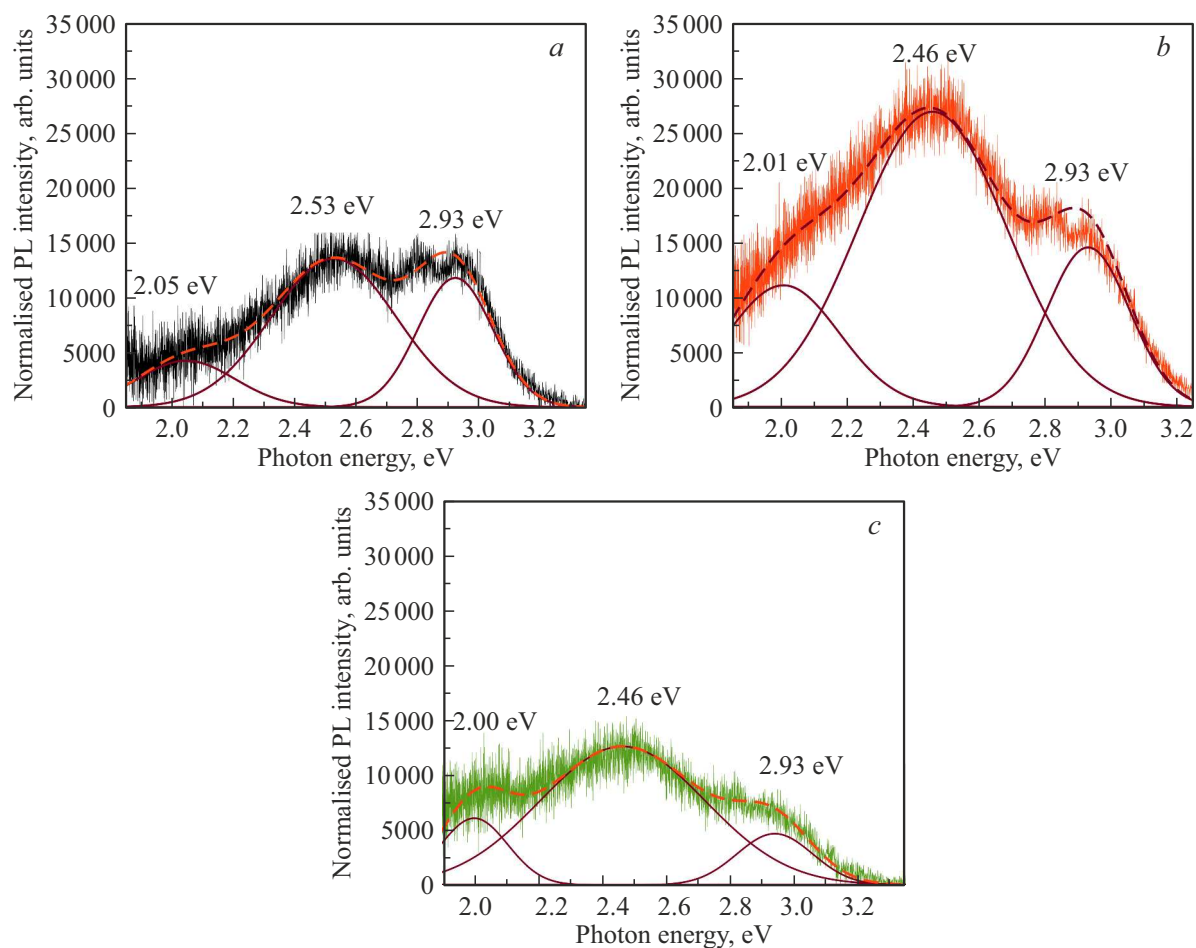
Figure 3. Decomposition of the PL spectra into Gaussian components for the initial sample (*a*) and the samples preliminarily irradiated with electrons (*b*) and ions (*c*).

and ions (curve *3*) is less than that of the initial sapphire sample (curve it1), that may indicate an increase in light absorption in the irradiated samples.

It is also seen from the Fig. 1 that all samples under study α-Al$_2$O$_3$ have a low-intensity luminescence band in the wavelength range $365-650$ nm ($1.9-3.4$ eV). The luminescence spectra in this range have a complex shape and consist of several broad components associated with the excitation of intrinsic defects in sapphire —neutral oxygen vacancies (*F*-centers) and aggregate centers in various charge states (F_2-, F_2^+-, F_2^{2+}- centers) [5–7]. It has been established [8,9] that, regardless of the methods of synthesis of α-Al$_2$O$_3$, it always has a lack of oxygen, which is confirmed by the presence of luminescence lines associated with oxygen vacancies, even in the initial sample (curve *1*). A similar PL spectrum was also observed in the study [10] for single-crystalline α-Al$_2$O$_3$.

It should be noted that the luminescence intensity of the sample pre-irradiated with electrons (curve *2* in Fig. 1) is greater than that of the initial sample in the entire wavelength range, while the intensity of the peak at the

wavelength $\lambda_{max} = 420$ nm (2.9 eV) decreases after the Al$_2$O$_3$ sample is irradiated with Ar$^+$ ions.

For the convenience of analysis, each of the PL spectra was decomposed into Gaussian components. To do this, the PL spectrum was converted to the energy scale [11], where the intensity was calculated by the formula $I(E) = I(\lambda)\frac{\lambda^2}{hc}$, after which the decomposition into Gaussian components was carried out. The Figure 3 shows the decomposition results for the initial sample (*a*) and the samples previously irradiated with electrons (*b*) and ions (*c*).

As can be seen from the Fig. 3, three Gaussian components were used to approximate the experimentally observed PL spectra of the α-Al$_2$O$_3$ samples. According to the literature data, the band with the maximum position $\lambda_{max} = 423$ nm (2.93 eV) observed in the PL spectra of all samples can be interpreted as the *F* center emission band, which is one of the main types defects in the sapphire anion sublattice and is a neutral oxygen vacancy, which has captured two electrons [5]. The dip observed in the spectrum in the 430 nm region can be associated with intense absorption of the emitted light by impurity Cr^{3+} ions, since the emission band of the *F* center overlaps

with one of the absorption bands of Cr^{3+} ions (transition $^4A_2 \to ^4T_1$) [12]. It is also possible that this dip is a measurement artifact. The ratios of the integrated intensities of the F-center bands obtained from the PL spectra for the initial sample and samples preliminarily irradiated with electrons and ions are $S_{el}/S_{init} \approx 1.29$ and $S_{ion}/S_{init} \approx 0.40$.

The emission band $\lambda_{max} = 500$ nm (2.48 eV) observed in the spectra cannot be interpreted unambiguously. In the literature this band is associated either with the emission of interstitial Al_i^+-centers with a maximum at 516 nm (2.4 eV) [13,14], or with the emission of F_2-centers, which are two neutral anion vacancies located at neighboring nodes, which have captured four electrons [15,16]. In the study [17] the 520 nm emission band was observed for α-Al_2O_3:Mg crystals and associated with the formation in $F_2^{2+}(2Mg)$ complex defect crystal, which represents two positive F^+ oxygen vacancies compensated by two Mg^{2+} ions.

Decomposition of the spectrum into Gaussian components shows that the position of this line in the PL spectrum shifts slightly towards lower energies (longer wavelengths) after irradiation with both electrons and ions. For the initial sample $E = 2.53$ eV ($\lambda_{max} = 489$ nm), for pre-irradiated samples $E = 2.46$ eV ($\lambda_{max} = 504$ nm). This may indicate that this band is a composite one: after preliminary irradiation, the intensity of the longer-wavelength component increases. Therefore, it seems most probable that the luminescence at 500 nm can be associated both with F_2 centers and with the presence of $F_2^{2+}(2Mg)$.

The formation of F_2 centers in sapphire is usually observed in oxides with a high concentration of oxygen vacancies, which are formed, for example, during high-temperature treatment of samples [15,18] or after their irradiation with neutrons, heavy ions, or high-energy electrons. energy [5,19,20]. In our case this band is observed even in the spectrum of the initial sample, which may indicate a rather large number of anion vacancies in the initial sapphire crystal. It can be seen from the Fig. 3,*a* that the observed PL bands of single and aggregate F-type centers are characterized by similar intensities, which indicates the presence of F-centers and their aggregates in crystals in close concentrations.

The integrated intensity of the band for the ion-irradiated sample increases insignificantly ($S_{ion}/S_{init} \approx 1.22$), while for the electron-irradiated crystal it increases by more than 2 times ($S_{el}/S_{init} \approx 2.22$).

Low-energy electron irradiation cannot lead to the generation of new defects in the samples under study, but it can stimulate the formation of electron-hole pairs and change the charge state of trapping centers and recombination. During electron irradiation of the crystal, first shallow (up to 0.1 eV below the bottom of the conduction band) and then deep traps associated with various kinds of defects contained in the initial sapphire sample are filled with electrons. After switching-off the electron irradiation, shallow traps are quickly released due to the thermal energy of the crystal and the electric field of the charge embedded in the dielectric,
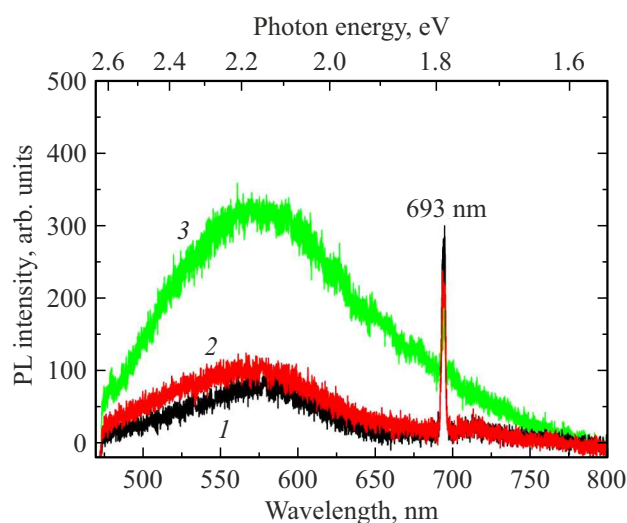

Figure 4. PL spectra of samples α-Al_2O_3 recorded at laser excitation wavelength $\lambda = 455$ nm. Curve *1* — initial sapphire sample, *2* — sample pre-irradiated with electrons, *3* — sample after irradiation with Ar^+ ions.

while the charge relaxation time in deep traps at room temperature can be measured in days and weeks [2].

The subsequent emptying of electron traps under the action of light leads to the transition of electrons to the conduction band of the crystal, as a result of which the probability of their capture by emission centers increases, and the number of radiative recombination events at emission centers increases.

Thus, the increase in intensity observed in the PL spectra at a wavelength of 420 nm can occur as a result of the capture of an electron from the conduction band by the F^+ center with the formation of an F center in an excited state and subsequent radiative relaxation of this state according to reaction

$$F^+ + e = F^* = F + h\nu.$$
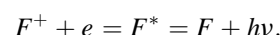
Similarly, the reaction can respond for the increase in the band intensity at 493 nm

$$F_2^+ + e = F_2^* = F_2 + h\nu.$$
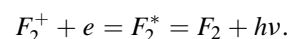
In the PL spectra of ion-irradiated samples the peak intensity $\lambda_{max} = 423$ nm (2.93 eV) decreases compared to the initial sample, that may be caused by the ionization of F-centers in the course of ion irradiation (neutralization of the positive ion Ar^+ as a result of its capture of an electron from the F-center).

The nature of the appearance of the PL band observed in the spectra of all samples at 590 nm is not entirely clear. It should be noted that this band was also observed in the spectra of single-crystalline α-Al_2O_3 by other authors, for example, in the study [10]. It is possible that the appearance of a peak at these wavelengths is associated with the absorption of radiation by impurity Cr^{3+} ions.

PL spectra upon excitation at a wavelength $\lambda_{ex} = 445\,nm$ Figure 4 shows the PL spectra of sapphire samples obtained with an Ntegra Spectra NT-MDT confocal microscope at an excitation wavelength of $\lambda_{ex} = 445$ nm. As noted above, this technique allowed to obtain PL data only from the near-surface layer of the sample with a thickness of no more than $2\,\mu$m, which minimized the effect of the unirradiated crystal part.

The PL spectra of these samples are a broad peak centered at the wavelength $\lambda_{max} = 570$ nm, on which a narrow peak is observed at $\lambda_{max} = 693$ nm, related as already noted, with impurity PL of Cr^{3+} ions.

It can be seen from the Fig. 4 that the PL intensity from pre-irradiated samples is higher than for the initial sapphire sample. In the case of an electron-irradiated sample, the integrated PL intensity increases by a factor of 1.5. In this case an increase in the PL intensity is observed mainly in the wavelength range $470-570$ nm. This may indicate the formation of additional emission centers associated with the formation of oxygen vacancies and their complexes in a thin near-surface sample layer. Indeed, despite the fact that aluminum oxide has a high radiation resistance, that allows it to be used in many areas of radiation physics, in particular in dosimetry, there are experimental data that under the action of low-energy electron bombardment $(1-3\,\text{keV})$ the surface of Al_2O_3 oxide can be destroyed due to electron-stimulated desorption of oxygen [21]. To explain the destruction mechanism of Al_2O_3, the Knotek–Feibelman [22] model developed for oxides with the maximum degree of valency was used. However, the cross section of the process of electron-stimulated desorption for sapphire is small and at an energy of incident electrons $2\,\text{keV}$ according to the data [20] is $2.7 \cdot 10^{-22}$ cm^2.

After irradiation of sapphire with Ar^+ ions, an increase in the integrated PL intensity in the wavelength range of $470-670$ nm by a factor of 4.1 is observed. According to the results of the calculation performed using SRIM [23] software, the depth of Ar^+ ions run with the energy $9\,\text{keV}$ in a monocrystal Al_2O_3 is about 10 nm. Thus, the observed significant increase in the PL intensity indicates the generation of new defects in this near-surface region under ion bombardment.

Conclusion

The PL spectra of the initial sample of single-crystalline sapphire and samples previously irradiated with electrons and low-energy ions were obtained using a confocal microscope with an excitation wavelength of 445 nm, as well as in a standard (nonconfocal) geometry with excitation at a wavelength of 355 nm. The PL spectra of all samples, including the initial sample, show lines associated with intrinsic defects in the crystal —neutral oxygen vacancies and their complexes, as well as impurity defects –Cr^{3+} ions. The observed spectra indicate the presence of a fairly large number of intrinsic defects in the crystals, especially in the crystal near-surface region.

Preliminary ion irradiation results in the disordering of the sample near-surface region, that manifests itself in a significant increase in the PL intensity in the wavelength range $500-750$ nm. Preliminary electron irradiation damages the sample near-surface region to a much lesser extent; however, it can lead to a change in the charge state of the defects which initially exist in the crystal, that is reflected in an increase in the intensity of the PL bands from these samples.

Conflict of interest

The authors declare that they have no conflict of interest.

References

[1] E.I. Rau, A.A. Tatarintsev, E.Yu. Zykova, I.P. Ivanenko, S.Yu. Kupreenko, K. F. Minnebaev, A.A. Haidarov. Phys. Solid State, **59** (8), 1526 (2017). DOI: 10.1134/S1063783417080212.

[2] E.I. Rau, A.A. Tatarintsev. FTT, **63** (4), 483 (2021). (in Russian). DOI: 10.21883/EOS.2022.09.54827.3397-22 [E.I. Rau, A.A. Tatarintsev. Phys. Solid State, **63** (4), 574 (2021). DOI: 10.1134/S1063783421040181].

[3] E.I. Rau, A.A. Tatarintsev, E.Yu. Zykova. Nucl. Instr. and Meth. in Phys. Res. B, **460**, 141 (2019). DOI: 10.1016/j.nimb.2018.12.030

[4] D.I. Bletskan, V.Y. Bratus', A.R. Luk'yanchuk, V.T. Maslyuk, O.A. Parlag. Tech. Phys. Lett., **34**, 612 (2008). DOI: 10.1134/S1063785008070237.

[5] B.D. Evans, G.J. Pogatshnik, Y. Chen. Nucl. Instr. and Meth. in Phys. Res. B, **91**, 258 (1994). DOI: 10.1016/0168-583X(94)96227-8

[6] M. Rodriguez, G. Denis, M. Akselrod, T. Underwood, E. Yukihara. Radiation Measurements, **46**, 1469 (2011). DOI: 10.1016/J.RADMEAS.2011.04.026

[7] V.S. Kortov, V.A. Pustovarov, T.V. Shtang. Radiation Measurements, **85**, 51 (2016). DOI: 10.1016/J.RADMEAS.2015.12.009

[8] H. Arendt, J. Hulliger. *Crystal Growth in Science and Technology* (Plenum Press., New York, 1989), p. 275–302. DOI: 10.1007/978-1-4613-0549-1

[9] R. Mogilevsky, S. Nedilko, L. Sharafutdinova, S. Burlay, V. Sherbatskii, V. Boyko, S.D. Mittl. Opt. Mater., **31**, 1880 (2009). DOI: 10.1016/J.OPTMAT.2008.11.023

[10] A.I. Kostyukov, A.V. Zhuzhgov, V.V. Kaichev, A.A. Rastorguev, V.N. Snytnikov, V.N. Snytnikov. Optical Materials, **75**, 757 (2018). DOI: 10.1016/J.OPTMAT.2017.11.040

[11] Y. Wang, P.D. Townsend. J. Luminescence, **142**, 202 (2013).
DOI: 10.1016/j.jlumin.2013.03.052

[12] E. Liver. *Elektronnaya spektroskopiya neorganicheskih soedineniy* (Mir, M., 1987), p. 2. (in Russian).

[13] J. Valbis, N. Itoh. Radiat. Eff. Defects Solids, **116**, 171 (1991).
DOI: 10.1080/10420159108221357

[14] A.I. Surdo, V.A. Pustovarov,V.S. Kortov, A.S. Kishka, E.I. Zinin. Nucl. Instrum. Methods Phys. Res. Sect. A: Accel. Spectrom. Detect. Assoc. Equip., **543**, 234 (2005).
DOI: 10.1016/j.nima.2005.01.189

[15] I. Tale, T.M. Piters, M. Barboza-Flores, R. Perez-Salas, R. Aceves, M. Springis. Radiat. Prot. Dosim., **65**, 235 (1996).
DOI: 10.1093/OXFORDJOURNALS.RPD.A031630

[16] V.S. Kortov, S.V. Zvonarev, A.I. Medvedev. J. Lumin., **131**, 1904 (2011). DOI: 10.1016/j.jlumin.2011.05.006

[17] M.S. Akselrod, A.E. Akselrod, S.S. Orlov, S. Sanyal, T.H. Underwood. J. Fluorescence, **13** (6), 503 (2003).
DOI: 10.1023/B:JOFL.0000008061.71099.55

[18] S.V. Soloviev, I.I. Milman, A.I. Surdo. Phys. Solid State, *54* (4), 683 (2012). DOI: 10.1134/S1063783412040270

[19] K.S. Jheeta, B.C. Jain, Ravi Kumar, K.B. Garg. Ind. J. Pure Appl. Phys., **46**, 400 (2008).

[20] M.F. Zhang, H.L. Zhang, J.C. Han, H.X. Guo, C.H. Xu, G.B. Ying, H.T. Shen, N.N. Song. Physica B, **406** (3), 494 (2011). DOI: 10.1016/j.physb.2010.11.021

[21] O.V. Rakhovskaya, S.S. Elovikov, E.M. Dubinina, E.S. Shakhurin, A.P. Dementjev. Surf. Sci., **274**, 190 (1992). DOI: 10.1016/0039-6028(92)90113-K

[22] M.L. Knotek, P.J. Feibelman. Phys. Rev. Lett., **40**, 964 (1978).
DOI: 10.1103/PhysRevLett.40.964

[23] The Stopping and Range of Ions in Matter Software. URL: http://www.srim.org